Fine-scale Horizontal Structure of Arctic Mixed-Phase Clouds

M. Rambukkange[1], J. Verlinde[1], E. Eloranta[2], E. Luke[3], P. Kollias[3] and M. Shupe[4]

[1]Penn State University, [2]University of Wisconsin, [3]Brookhaven National Laboratory,
[4] CIRES and NOAA-ETL
(Corresponding author: J. Verlinde, 502 Walker Building, Pennsylvania State University, University Park, PA 16802. e-mail: verlinde@essc.psu.edu. Phone: (814) 863-9711)

1. Introduction

Recent in situ observations in stratiform clouds suggest that mixed phase regimes, here defined as limited cloud volumes containing both liquid and solid water, are constrained to narrow layers (order 100 m) separating all-liquid and fully glaciated volumes (Hallett and Viddaurre, 2005). The Department of Energy Atmospheric Radiation Measurement Program's (DOE-ARM, Ackerman and Stokes, 2003) North Slope of Alaska (NSA) ARM Climate Research Facility (ACRF) recently started collecting routine measurement of radar Doppler velocity power spectra from the Millimeter Cloud Radar (MMCR). Shupe et al. (2004) showed that Doppler spectra has potential to separate the contributions to the total reflectivity of the liquid and solid water in the radar volume, and thus to investigate further Hallett and Viddaurre's findings.

The Mixed-Phase Arctic Cloud Experiment (M-PACE) was conducted along the NSA to investigate the properties of Arctic mixed phase clouds (Verlinde et al., 2006). We present surface based remote sensing data from M-PACE to discuss the fine-scale structure of the mixed-phase clouds observed during this experiment.

2. Data

During the period Oct. 4-8, 2006, the NSA was under disturbed synoptic conditions producing complex cloud structures over the ACRF site at Barrow. The lowest atmospheric layers (< 1.5 km) were characterized by flow from the east-northeast with considerable fetch over the Arctic Ocean. Above this layer, separated by a strong inversion, was the remnant of a small decaying lee-side low. Figure 1 shows the dry and dew point temperatures and horizontal wind component profiles through the lower 5 km of the atmosphere at 1700 UTC on the 6th. These profiles reveal that several water saturated layers were encountered during the ascent.

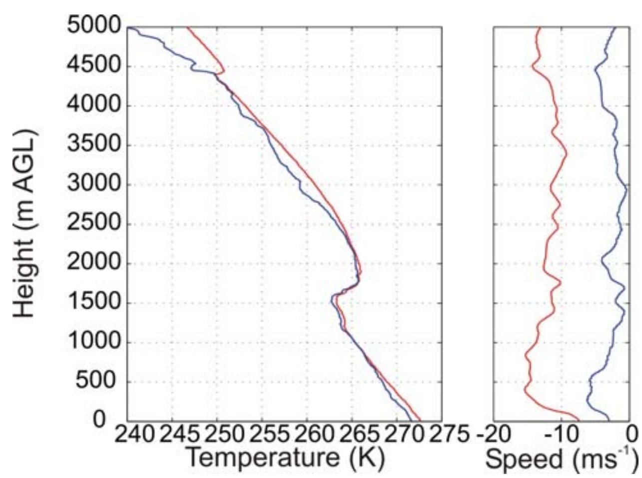

Figure 1: The atmospheric sounding for Barrow 1700 UTC 6 October 2004. The blue and red lines are the temperature and dew point on the left-hand panel, and the u and v wind components on the right-hand panel.

Figure 2 shows profiles from the MMCR and the Arctic High Spectral Resolution Lidar linear depolarization (AHSRL; Eloranta, 2005), revealing the complicated, multilayer structure of clouds over the site. Although the trained eye may see some indications of layering in the radar reflectivity, it is impossible to identify much of the structure in the layer. The lidar depolarization reveals more of the layer

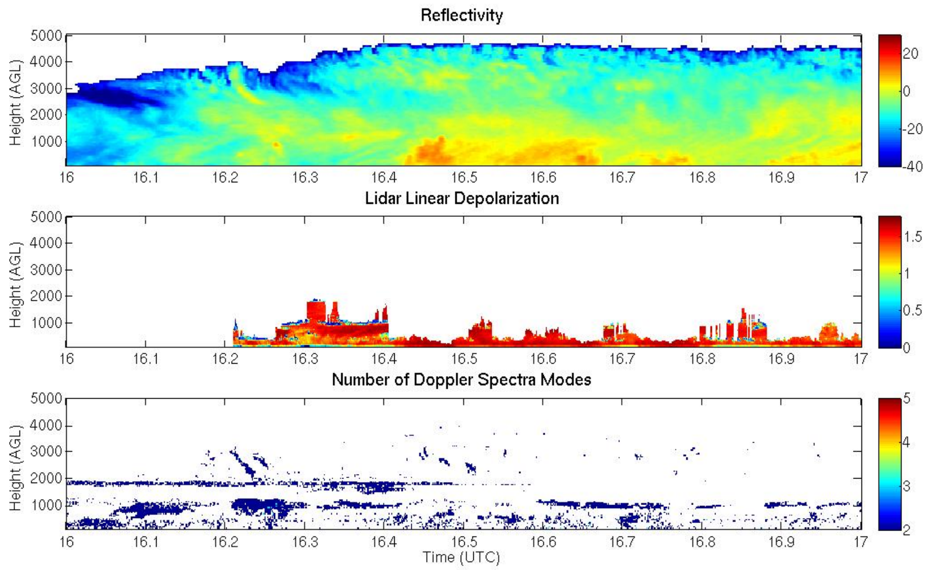

Figure 2: Reflectivity (dBZ) from the MilliMeter Wave Radar (MMCR), linear depolarization (log(Percentage Depolarization)) from the Arctic High Spectral Resolution Lidar (AHRSL), and the number of modes identified in the Doppler velocity spectra over Barrow, Alaska on 6 October 2004.

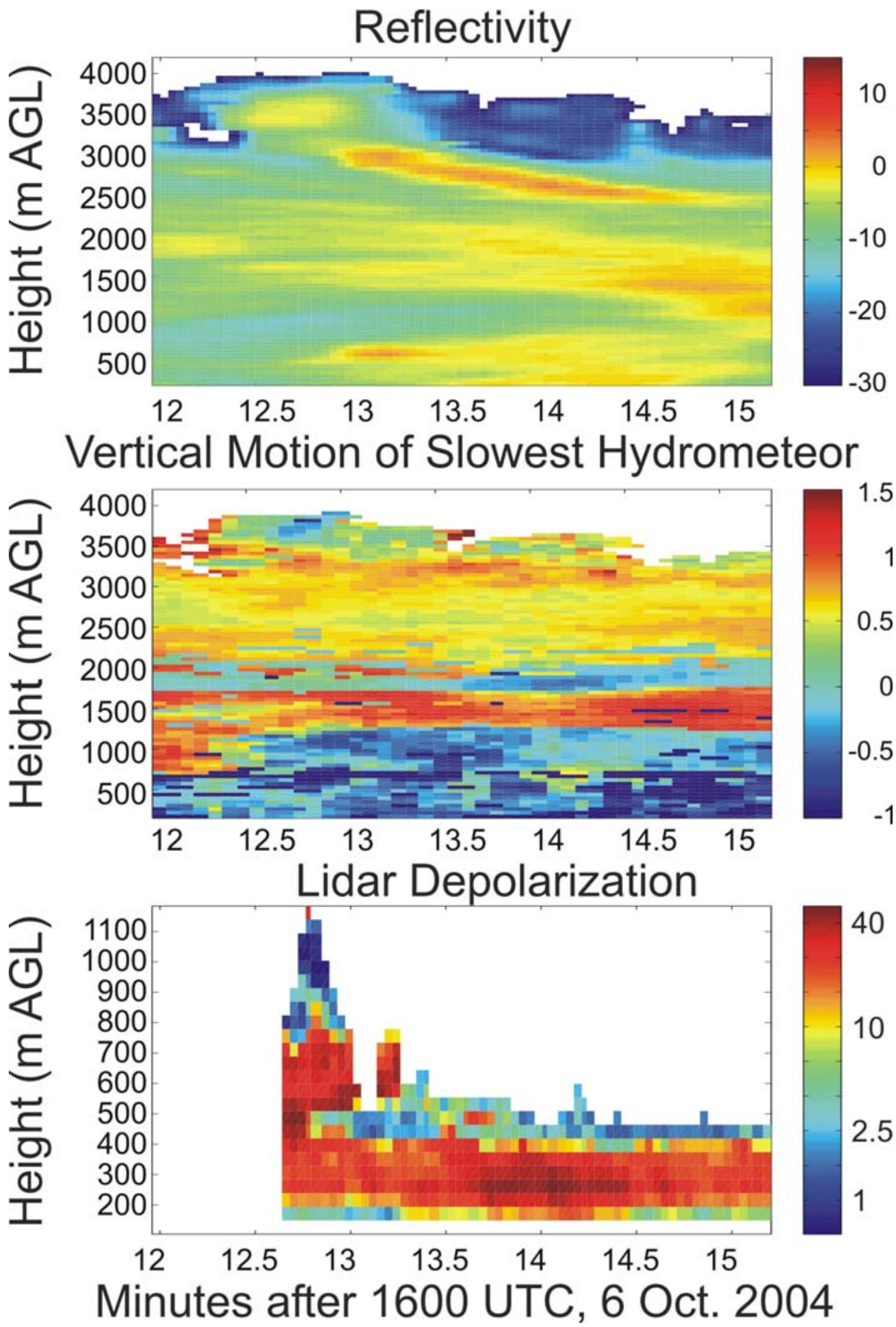

Figure 3: Reflectivity (dBZ) from the MilliMeter Wave Radar (MMCR), fall velocity (ms^{-1}) of the slowest falling particles determined from the Doppler velocity power spectra, and the linear depolarization (log(Percentage Depolarization)) from the Arctic High Spectral Resolution Lidar (AHRSL) over Barrow, Alaska on 6 October 2004.

structure. Multiple patchy liquid layers are visible below 1 km, with indications of more persistent layers above, although these are mostly obscured by attenuation of the lidar beam by the lower liquid layers.

The spectral processing routine from Luke et al. (2006) identifies multi-modal Doppler spectra, the number of modes of which is displayed in Fig. 2c. Comparing these with the lidar depolarization reveals a strong correlation between locations of these multi-modes and the presence of low lidar depolarization, or liquid water. This is further confirmed by comparing the heights where these multi-modes occur with the water saturated layers in Fig. 1.

3. Spectral Analysis

The correlation between Doppler spectra multi-modes and low lidar linear depolarization warranted a closer look at the spectra. We selected a 3 minute period during which both a layered and slanting multi-mode structures were observed (1612-1615 UTC) to do a detailed analysis of the spectra. Each Doppler velocity spectrum was threshold on the noise floor, and the velocity of the slowest falling (detected) hydrometeor was identified. In cloud, where the slowest falling hydrometeors may be assumed to fall with terminal fall speeds below the velocity resolution of the Doppler spectrum, this velocity may be assumed to correspond to the vertical velocity of the air in the volume. In precipitation, it is the fall velocity of the slowest precipitation particles added to an unknown air vertical velocity.

Figure 3 presents the reflectivity, velocity of the slowest hydrometeor, and lidar linear depolarization for the selected three minute period. Comparing to the same period in Fig. 2c, one see that the slanted multi-mode structure is associated with the slanting higher reflectivity feature, a precipitation shower, whereas the linear multi-mode structure has no perceptible reflectivity structure associated with it.

Looking at the velocity field (Fig. 3b) more features can be distinguished. Updrafts, here identified as negative velocities, are visible in the small reflectivity structure at cloud top. This 500 m deep cloud has a tilted updraft structure, with the precipitation falling on the down shear (~12.2 min) side of the cloud. The jump in velocity along the horizontal line between 3.4 and 3.5 km suggest that the base of this cloud layer is at approximately this height. This cloud layer consists of multiple smaller cells, each producing its own precipitation shaft.

The linear multi-mode structure is closely associated with a distinct horizontal anomaly in the vertical velocity field (1.7 – 2.2 km). The magnitude varies between 1 ms^{-1} up and .5 ms^{-1} down over a 1.2 minute period in the highly stable inversion layer (Fig. 1). There is another abrupt change (more than 1 ms^{-1}) in fall velocity below that layer, suggesting that another cloud base was passed. The vertical velocities in the boundary layer coming of the ocean (z<1 km) are generally positive, although there are good indications that there is contamination in the spectra.

Figure 4 displays Doppler velocity power spectra for the selected time period. Each panel represents a single height: the color contours at a given time indicate the power returned of particles of given vertical motion. The integral over the power spectrum at a given height and time represents the total reflectivity in the beam. Here we display spectra starting at 1590 m, below the linear multi-modal structure, through 3030 m, approximately at the top of the precipitation shaft.

Two distinct domains can be identified in height. Above 2220 m, there is little variation in velocity of background precipitation, and the observed multi-modality derived from the

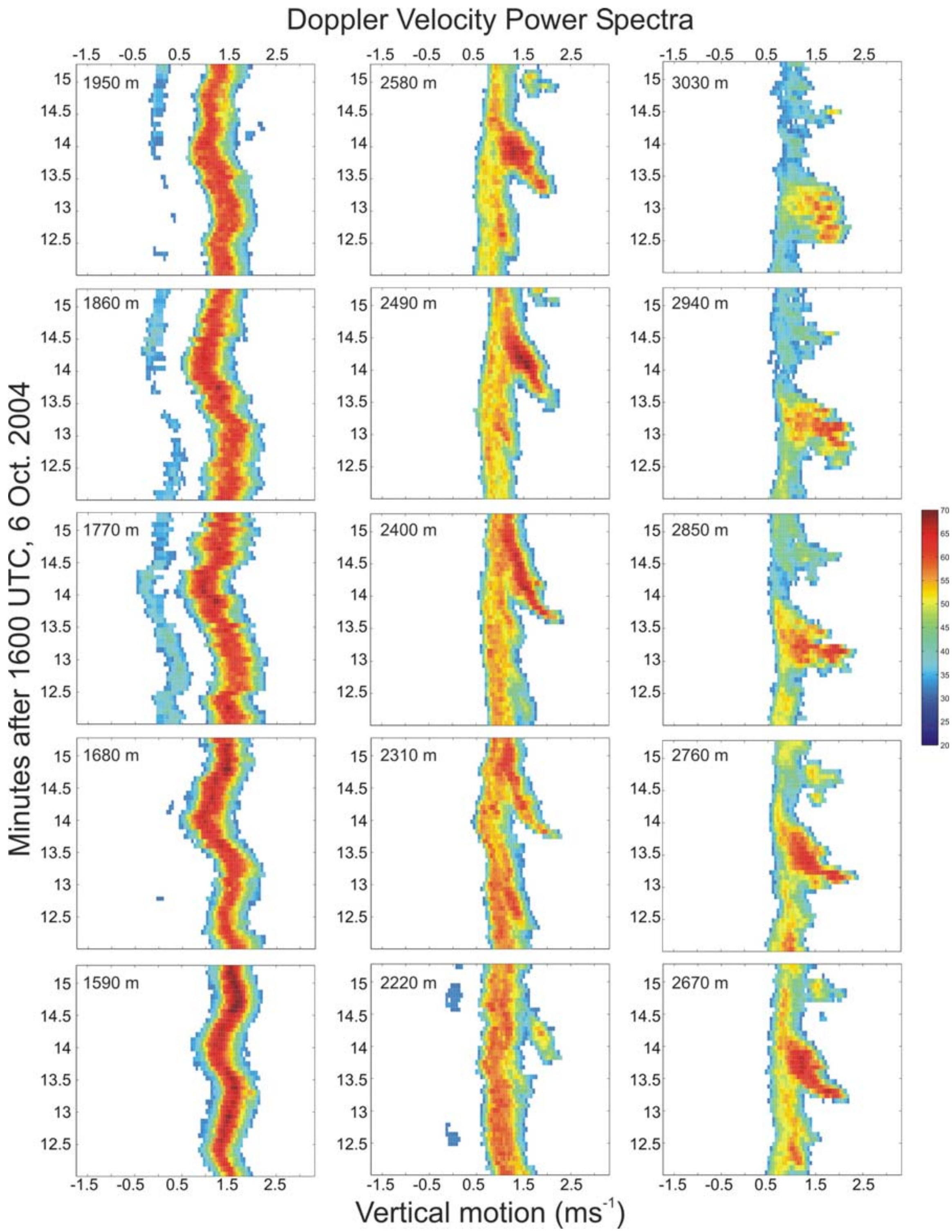

Figure 4: Doppler velocity power spectra at various heights over Barrow Alaska 6 October 1004. Each panel represents spectra at the stated height (indicated in the left upper corner) for the ~3 min period 1612 UTC to 1615 UTC. See text for discussion on the interpretation of the spectrographs.

precipitation showers. Below 2220 m, in the very stable layer just above the inversion and into the inversion layer, wave-like variations in the velocity of the background precipitation is easily observable. We suggest that these waves are gravity waves resulting from boundary convection, in the cold air flowing of the ice pack over a fetch of open water, impinging on the stable layer above.

The bimodality in the spectra through the heights 1680 m – 2220 m is clearly evident, and is the result of two distinct, and persistent in time, populations in fall velocity space. The mean air motion is common to all the particles in the volume, therefore one can easily seen that the higher reflectivity population falls with a mean terminal velocity approximately 1 ms^{-1} faster than the lower reflectivity population. Careful analysis reveals that the separation in fall speed between the two populations increase from about 0.9 ms^{-1} at 2220 m to about 1.3 ms^{-1} at 1770 m, associated with a general increase in spectral reflectivity, suggesting that these particles are growing as they are falling through this layer. We associate the slower falling population with the cloud itself, and speculate that it is the liquid drops. This speculation is supported by the low linear depolarization observed by the lidar at few minute later (Fig. 2b) and the water saturation in the sounding at these levels. In situ observations by the UND Citation also detected liquid at this level, although somewhat later in the day (Zhang et al., 2006). Combining these panels with Fig. 2, one can then see that this liquid layer persisted in the presence of persistent ice precipitation.

Also observable in the spectra at heights 1770 m – 1950 m are evidence of turbulence. This can be seen as shifts in the spectra for successive times, particularly in the positive (downward) extensions of the waves. The profiles of spectra and the atmospheric thermodynamic sounding suggest that the cloud is not a single continuous layer, but rather several, thin layers. Evidence of this can be seen in Fig. 3b, where in the gravity wave downward displacement (12.4 – 13.2 min) pixels with higher downward velocities are evident. When such layers are vertically displaced, the atmosphere may develop absolute instabilities because of differences in the dry and moist adiabatic lapse rates, giving rise to convective overturning in those layers.

Turning to the layers above 2220 m, some evidence of wave activity can still be discerned, although the vertical velocity fluctuations are minor. Of greater interest is the precipitation fall streak, discernable as the protrusion from the background spectra. The progression of spectra with time and height allows one to develop a picture of the fall spectrum of the precipitating particles. Note the change in slope with height of the protrusion. This change in slope is the result of size sorting of the precipitation particles, with the faster falling hydrometeors arriving at lower heights well before the slower hydrometeors do.

This particular fall streak can be followed all the way down from 3030 m to 1950 m, where the last (or first!) hydrometeors are just discernable to the right of the background spectrum. Note that the velocity of fastest falling hydrometeors barely change with height. As the cloud is detectable at 1950 m, a good estimate for the terminal fall velocity of these hydrometeors can be found by looking at the difference between the left-most edge of the cloud spectrum and the fall velocity of the precipitation particles. This difference is 2.2 ms^{-1}, which in turn, suggest a general downward air motion of ~0.3 ms^{-1}. One sees then that the slowest falling hydrometeors fall with a terminal velocity of approximately 0.2 ms^{-1}. Moreover, the spectra at heights 2310 m – 2580 m two populations of hydrometeors, with mean fall velocities separated by ~0.2 ms^{-1}.

What is clear from these spectra is that the multiple modes observed associated with this fall streak are not associated with liquid cloud, but rather with different populations of ice hydrometeors. In situ observations taken during M-PACE (McFarquhar et al., 2005) reveal different types of ice crystals, including frozen drizzle, aggregates and pristine crystals. A more in depth analysis of these spectra with the in situ measurements are called for.

4. Conclusions

The Doppler velocity power spectra provided evidence that in Arctic mixed-phase clouds supercooled liquid layers can be maintained in the presence of ice precipitation, as was suggested by Harrington et al. (1999). This finding is in contrast to the in situ observations of Hallett and Viddaurre (2005) who found that mixed phase regimes in clouds are narrow.

References

Ackerman, T.P. and Stokes, G.M., 2003: The Atmospheric Radiation Measurement Program. *Physics Today*, **56,** 38-44.

Eloranta, E. W., 2005: High Spectral Resolution Lidar. *Lidar: Range-Resolved Optical Remote Sensing of the Atmosphere*, Klaus Weitkamp Ed, Springer Series in Optical Sciences, Springer-Verlag, 460 pp.

Hallett J. and G. Vidaurre, 2005: Characterization and Origin of Mixed Phase Cloud. AGU Fall Meeting, San Francisco, CA. A33E-02.

Harrington, J.Y, T. Reisin, W.R. Cotton, and S.M. Kreindenweis, 1999: Cloud resolving simulation of Arctic stratus. Part II: Transition season clouds, *Atmos. Res*. **51**, 45-75.

McFarquhar and Co-Authors, 2005: Assessing current parameterizations of mixed-phase clouds using in-situ profiles measured during the Mixed-Phase Cloud Experiment. 15th ARM Science Team Mtg., Daytona Beach, FL. (http://www.arm.gov).

Luke, E and Co-Authors, 2006: An automatic Doppler Spectrum Classifier for the MMCRs. 16th ARM Science Team Meeting. Albuquerque, NM. (http://www.arm.gov).

Shupe, M. D., P. Kollias, S.Y. Matrosov and T.L. Schneider, 2004: Deriving mixed-phase cloud properties from Doppler radar spectra. *J. of Atmos. Oceanic Technol.*, **21**, 660–670.

Verlinde, J. and Co-authors, 2006: The Mixed-Phase Arctic Cloud Experiment (M-PACE). Submitted to *BAMS*.

Zhang and Co-Authors, 2006: Microphysical properties of mixed-phase clouds sampled during the Mixed Phase Cloud Experiment (MPACE). 16th ARM Science Team Meeting. Albuquerque, NM. (http://www.arm.gov).